Mesomorphous Structure and Macroscopic Patterns Formed by Polymer and Surfactant from Organic Solutions

Shuizhu Wu,* Fang Zeng,* Hongping Zhu, Shaojin Luo, Biye Ren, and Zhen Tong

Department of Polymer Science & Engineering, South China University of Technology, Guangzhou 510640, China

Received May 22, 2005; Revised Manuscript Received August 1, 2005

ABSTRACT: Ordered mesomorphous structures were obtained from the ternary system of organic solvent, polymer, and surfactant, and this microscopic ordering could lead to unique water-wave-like macroscopic patterns in solid polymer−surfactant film. The mesomorphous structures and macroscopic patterns were obtained by dissolving a nonpolyelectrolyte polymer and cationic surfactant in organic solvents and casting the solutions on glass substrates. The patterns thus obtained are composed of concentric rings, and these concentric rings, with their diameters up to centimeters, alternatively consist of macroscopic convex ridges and concave valleys, with the former being amphormous phase and the latter being ordered mesomorphous one. This macroscopic patterning in a solid polymer−surfactant system could offer a new way for fabricating ordered supramolecular structure in macroscopic dimensions.

Introduction

Supramolecular structures generated through self-assembly have attracted great attention due to their enhanced materials properties.[1−4] The solid-state supramolecular structures formed by polyelectrolyte and surfactants through self-assembly also exhibit unique mechanical, optical, electrical, and biological properties.[1,2,5−8] A number of studies indicate that the strong interactions between the polyelectolytes and surfactants often result in highly ordered mesomorphous structures, e.g., nanoscale or micrometer-scale lamella and cylindrical structures, the less ordered bicontinuous sponge structure, and perforated layer structures.[1,5,9−14] However, for polymer−surfactant systems with no strong interaction involved, there is no report on the formation of highly ordered structure, and no macroscopic pattern has ever been constructed in solid-state polymer−surfactant systems.

In this paper, we report the formation of water-wave-like macroscopic patterns composed of concentric rings in solid polymer−surfactant film, which were obtained by dissolving a thiophene-containing polymer and cationic surfactant in organic solvents and casting the solutions on glass substrates. The concentric rings, with their diameters up to centimeters, consist of convex ridges and concave valleys, with the former being amphormous phase and the latter being ordered mesophase one. The factors that affect the macroscopic pattern formation were studied experimentally, and possible mechanisms for the formation of the mesomorphous structure as well as the macroscopic pattern were proposed.

Experimental Section

Materials. Thiophene-3-acetic acid, 3-hydroxy-4-methoxybenzaldehyde, methyl methacrylate, ethyl acrylate, tetraoctylammonium bromide (TOAB), tetrabutylammonium bromide (TBAB), tetradodecylammonium bromide (TDAB), dioctylsodium sulfosuccinate, and polyoxethylene sorbitan tristearate were purchased from Aldrich Chemicals. Piperidine and methacryloyl chloride were received from Acros Organics. Methyl methacrylate and ethyl acrylate were distilled before use. *N*,*N*-Dimethylformamide (DMF), toluene, acetone, and methanol were analytically pure solvents, and they were distilled before use. Tetrahydrofuran (THF) was dried over sodium/benzophenone and distilled just before use.

Synthesis of Thiophene Compound. Thiophene-3-acetic acid and 3-hydroxy-4-methoxybenzaldehyde in molar ratio 1:1 were dissolved in piperidine and refluxed overnight. After evaporating the solvent, the crude product was dissolved in methanol and filtered. Then methanol was removed under vacuum, the product was recrystallized in chlorobenzene and toluene (1:1 in volume), and a dark yellow crystalline solid was obtained.

Synthesis of Thiophene-Containing Monomer. To a solution of thiophene compound (0.02 mol) in 100 mL of anhydrous tetrahydrofuran at room temperature was added triethylamine (0.022 mol), and the solution was stirred for 15 min. The reaction mixture was cooled at 0 °C, and freshly distilled methacryloyl chloride (0.022 mol) in 10 mL of anhydrous tetrahydrofuran was added. The resulting mixture was allowed to warm to room temperature and stirred overnight. The reaction mixture was filtered. The product, obtained after evaporating the solvent, was washed with large amounts of hexane and methanol (4:1 in volume). Finally, a dark yellow solid was obtained. ^{1}H NMR (500 MHz, $CDCl_3$, 25 °C, TMS): δ (ppm), 6.9−7.5 (aromatic H), 5.7−6.2 (CH=CH), 5.0−5.1 (CH_2=), 3.6−3.8 (OCH_3), 1.8−2.0 (CH_3). FT-IR (KBr): 3100 cm^{-1} (ν_{CH} arom), 2980 and 2950 cm^{-1} (ν_{CH} aliph), 1715 cm^{-1} ($\nu_{C=O}$), 1610 cm^{-1} ($\nu_{C=C}$, aliph), 1510 cm^{-1} ($\nu_{C=C}$, phenyl), 1440 cm^{-1} (δ_{CH}, aliph), 1380 cm^{-1} ($\nu_{C=C}$, thiophenyl), 1250−1000 cm^{-1} (ν_{C-O}), 650−900 cm^{-1} (δ_{CH}, arom).

Polymerization of Thiophene-Containing Polyacrylate (TPA). 2 g (0.0067 mol) of the above thiophene-containing monomer was dissolved in dry dimethylformamide; 3 g (0.03 mol) of methyl methacrylate and 5 g (0.05 mol) of ethyl acrylate were added to the solution. The polymerization was carried out in the presence of azobis(isobutyronitrile) (AIBN, 1 wt %) as an initiator. The polymerization medium was outgassed twice before heating and stirring at 70 °C for 240 h under nitrogen. Then the polymerization mixture was poured into cold methanol. The isolated copolymer was redissolved in THF and precipitated in cold methanol, filtered, washed with deionized water, and finally dried under vacuum at 60 °C for 72 h. ^{1}H NMR (500 MHz, $CDCl_3$, 25 °C, TMS): δ (ppm), 7.0−7.4 (aromatic H), 6.6−6.8 (CH=CH), 4−4.2 (C(O)OCH_2), 3.5−3.73 (OCH_3, C(O)OCH_3), 0.9−2.2 (CH_3, backbone CH_2 and CH).

* To whom correspondence should be addressed: e-mail shzhwu@scut.edu.cn; Ph +86-20-83683721; Fax +86-20-87114649.

10.1021/ma051042g CCC: $30.25
Published on Web 10/07/2005

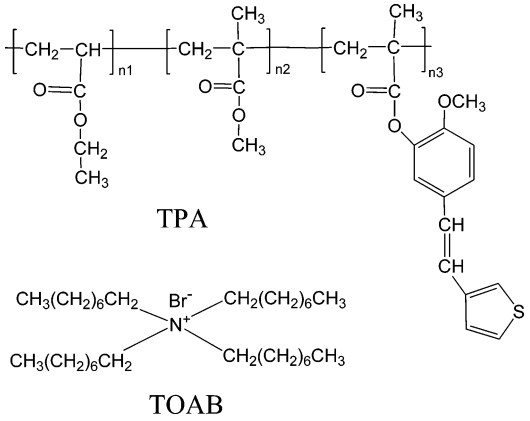

Figure 1. Molecular structure of the polymer and the surfactant TOAB.

FT-IR (KBr): 2980 and 2950 cm^{-1} (ν_{CH} aliph), 1735 cm^{-1} ($\nu_{C=O}$), 1640 cm^{-1} ($\nu_{C=C}$, aliph), 1530 cm^{-1} ($\nu_{C=C}$, phenyl), 1440 cm^{-1} (δ_{CH}, aliph), 1380 cm^{-1} ($\nu_{C=C}$, thiophenyl), 1250−1000 cm^{-1} (ν_{C-O}), 650−900 cm^{-1} (δ_{CH}, arom).

Film Preparation. The polymer−surfactant films were prepared as follows: the surfactant and the polymer TPA at a certain ratio were dissolved in an organic solvent (toluene, benzene, xylene, or acetone) to form a solution with the concentration of 6 wt %, a clear solution resulted, and then the solution was filtered through a 0.50 μm Teflon filter and cast on 2.5 cm × 4 cm glass substrates. Then a culture dish was covered over the glass substrate. Afterward, the films were allowed to dry in a thermostat at a constant temperature.

Characterization. FT-IR spectra were measured by using Nicolet Magna 760 FT-IR spectrometer. ^1H NMR spectra were recorded on a Varian Unity Inova 500 MHz NMR spectrometer. Molecular weight and molecular weight distribution were determined by a Waters gel permeation chromatograph with the 2410 RI detector. Polarizing micrographs were taken on a Zeiss Axiolab polarizing microscope. Small-angle X-ray scattering (SAXS) measurements were performed on Philips X'Pert PRO X-ray diffractometer (Cu Kα) (scattering vector $q = (4\pi/\lambda) \sin\theta$, where 2θ is the angle between the incident light and the scattered light). Differential scanning calorimetry (DSC) experiments were performed with 3−5 mg of samples in a 6 mm aluminum pan on a Netzsch DSC 204 under a nitrogen atmosphere at a heating/cooling rate of 5 °C/min. In the DSC measurements, for the polymer−TOAB system with the polymer content of 55 wt %, the solid film on the concave regions was carefully scraped off with a knife for the measurement, and all the samples were dried under vacuum at 60 °C for 72 h before DSC measurement. Elemental analysis was performed on a Vario EL elemental analyzer. For each elemental analysis, about 5 mg material was carefully taken from a convex region or a concave region of a film, so as to determine the nitrogen content of the materials.

Results and Discussion

The synthesized thiophene-containing polyacrylate (TPA) is a random acrylate copolymer with long pendant groups [2-methoxy-5-(2-thiophen-2-yl-vinyl)phenyl ester groups] (Figure 1). The molecular weight of the polymer, as characterized by gel permeation chromotography with polystyrene as the standard, is 3.1×10^4 with the polydispersity index of 2.9, and the glass transition temperature as determined by DSC for the polymer is 52 °C. The polymer and the surfactant were dissolved in toluene with an appropriate TPA to TOAB ratio, a transparent and dark-yellow solution was obtained, and then the solution was cast on glass substrate and was allowed to dry in a thermostat at varied temperatures; finally, a water-wave-like pattern composed of millimeter-to-centimeter scale concentric rings appeared

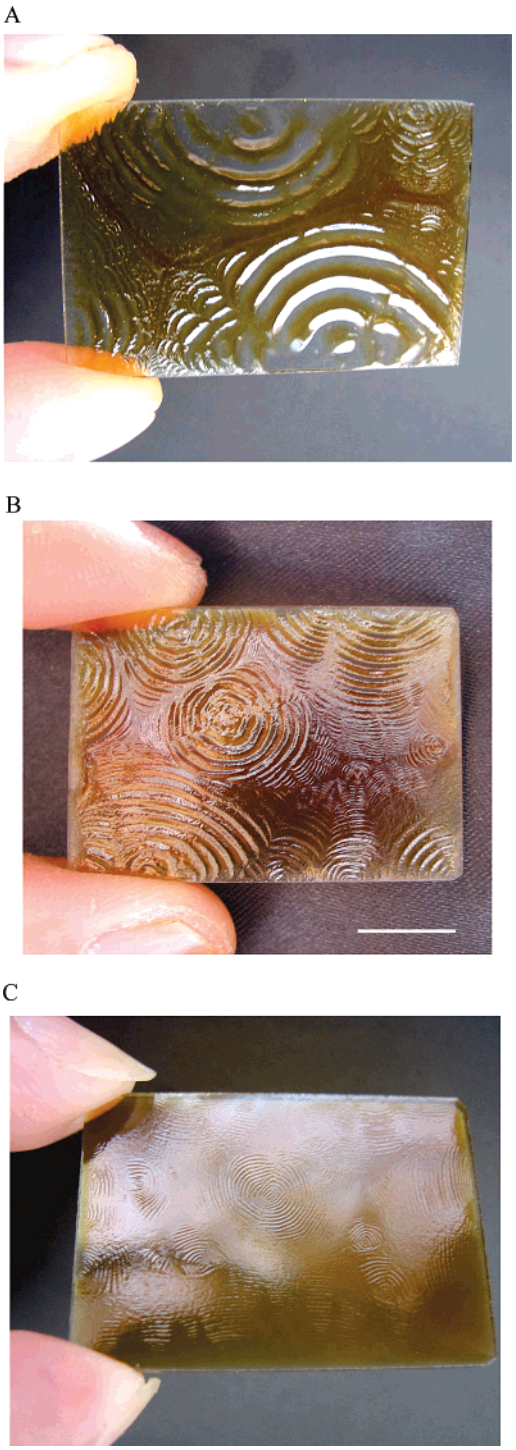

Figure 2. Photographs of the macroscopic patterns formed on 4.0 cm × 2.5 cm glass plates by polymer and surfactant with the polymer content of 55 wt % in the film; the solvent was toluene, and the amount of the polymer/TOAB solution cast on the glass was the same: (A) cast at 20 °C; (B) 25 °C, scale bar 1 cm; (C) 45 °C.

(Figure 2) during the solvent evaporation under appropriate conditions. We found that the removal of the thiophene-containing pendant groups results in the disappearance of macroscopic patterns.

Factors That Affect Formation of Macroscopic Pattern. The formation of the pattern was found to be dependent on several factors. Table 1 shows the effects of polymer content, the surfactant type, and the solvent type on the formation of the macroscopic pattern. First, the polymer content in the cast film was found to be

Table 1. Effects of Polymer Content in Solid Film, Solvent Type, and Surfactant Type on the Formation of a Macroscopic Pattern[a]

	solvent[b]				surfactant[c]		
polymer content (wt %)	acetone	benzene	toluene	xylene	TBAB	TOAB	TDAB
10	○	○	○	○	○	○	○
25	○	○	⊙	⊙	○	⊙	○
55	⊙	⊙	●	●	○	●	○
65	⊙	⊙	●	●	○	●	○
75	⊙	⊙	⊙	⊙	○	⊙	○
80	○	○	○	○	○	○	○
90	○	○	○	○	○	○	○

[a] The films were cast at 25 °C; ○, no pattern formed; ⊙, poorly formed macroscopic pattern; ●, well-formed macroscopic pattern. [b] For solvent effects investigation, TOAB was used as the surfactant. [c] For surfactant effects investigation, toluene was used as the solvent. TOAB: tetraoctylammonium bromide; TBAB: tetrabutylammonium bromide; TDAB: tetradodecylammonium bromide.

critical to the pattern formation. For the TPA−tetraoctylammonium bromide (TOAB) system, no matter what solvent was used, as the weight percentage of the polymer was low (10 wt %), no macroscopic pattern appeared in the solid polymer−surfactant film as the solvent evaporates. As the weight percentage of polymer reached 25% in the solid film, poorly formed patterns could be observed, and the large and well-formed pattern could be observed as the polymer content was increased to around 55 wt % in the solid film when toluene or xylene was used as the solvent, as shown in Figure 2; when the amount of polymer in the solid film was too high (80 wt % or higher), no macroscopic pattern could be observed as well.

As for the surfactant, we used three cationic surfactants with symmetrical structure. They were tetrabutylammonium bromide (TBAB), tetraoctylammonium bromide (TOAB), and tetradodecylammonium bromide (TDAB). These surfactants all have four identical alkyl tails; only the number of carbons in the alkyl tails for these surfactants is different. However, we could only obtain macroscopic patterns by using TOAB which has eight carbon atoms in each tail. No macroscopic patterns could be observed for the TPA−TBAB systems or the TPA−TDAB systems, no matter what solvent was used. Hence, the length of the alkyl tails of the surfactant has great effects on the structure formation of the polymer−surfactant systems. We also tried other oil-soluble surfactants with asymmetrical structure, such as anionic surfactant dioctylsodium sulfosuccinate (aerosol OT) and nonionic surfactant polyoxethylene sorbitan tristearate (Tween), and no pattern was observed on the polymer−surfactant films.

In addition, several solvents with different boiling temperatures were also employed to prepare the TPA−TOAB solid films. As for the low-boiling-point solvents (e.g., acetone and benzene), when the polymer content is between 55 and 75 wt %, only poorly formed macroscopic patterns could be generated. While for the high-boiling-point solvents (toluene and xylene), when the polymer content is at 55 or 65 wt %, well-formed macroscopic patterns could appear as the solvent evaporated, as indicated in Table 1.

The final circular pattern in the solid films was also affected by the film-forming temperature. When the solid films were obtained by drying at 45 or 20 °C instead of room temperature (25 °C), obvious changes in the circular patterns were observed (see Figure 2). Photographs of the resultant circular patterning (Figure 2) in the solid polymer−surfactant films show that, as the film-forming temperature increases, the ring dimension of the patterns becomes smaller and both the ring thickness and the inter-ring spacing become lower. We suppose the pattern formation needs the cooperative motion (or migration) of both polymer chains and surfactant molecules during the solvent evaporation, and at higher film-forming temperature fast solvent evaporation speed makes the solvent leave more quickly; hence, the motion of polymer chain segments could be frozen more quickly, and the concentric rings could not "grow" to thicker ones. We also found that, as the film-forming temperature was further increased to 50 °C or reduced to 15 °C, we could only obtain transparent films with no patterns on them. So the rough temperature range for the pattern formation is 20−45 °C.

Polarizing Optical Micrographs. We selected some patterns with small rings to observe their morphologies on the polarizing optical microscope. Parts A and B of Figure 3 show the morphology for a same area of a pattern under parallel-polarized light and perpendicular-polarized light, respectively, in which the stripes represent a part of rings. Figure 3C shows morphology for a part of a larger concentric ring under perpendicular-polarized light, while Figure 3D shows the central part of a concentric ring under perpendicular-polarized light. By comparing parts A and B of Figure 3, we can find that each brighter stripe in Figure 3A corresponds to one bright stripe in Figure 3B. Since under the parallel-polarized light (similar to unpolarized light) the thinner regions of a film absorb less light, the brighter stripes in Figure 3A represent the concave valleys, while in Figure 3B, bright stripes represent anisotropic structure. So, it can be found that only the concave valleys of the film can transmit the perpendicular-polarized light, while the ridges cannot; this indicates that the convex ridges mostly contain the isotropic (amorphous) structure, while the concave valleys mainly comprise the ordered anisotropic structure. For the same reason, the three bright arc stripes in Figure 3C correspond to three valleys (ordered structure) in a larger pattern, and the center point of the rings consists of the ordered structure, as shown in Figure 3D. Thus, it can be concluded that the concentric rings in the film are organized alternatively by macroscopic circular amorphous regions and ordered regions. In addition, a few crystalline domains of residual surfactant can be seen in Figure 3A,B; it is obvious that the pure surfactant crystalline domains are different compared with the ordered structure in the concave regions. On the other hand, we could not observe any bright stripe for the films with no macroscopic pattern.

To further confirm that the concave regions mainly consist of the ordered anisotropic structure and the convex regions mainly consist of amorphous structure, a part of the concentric ring was observed on the polarizing optical microscope as the polarizers were

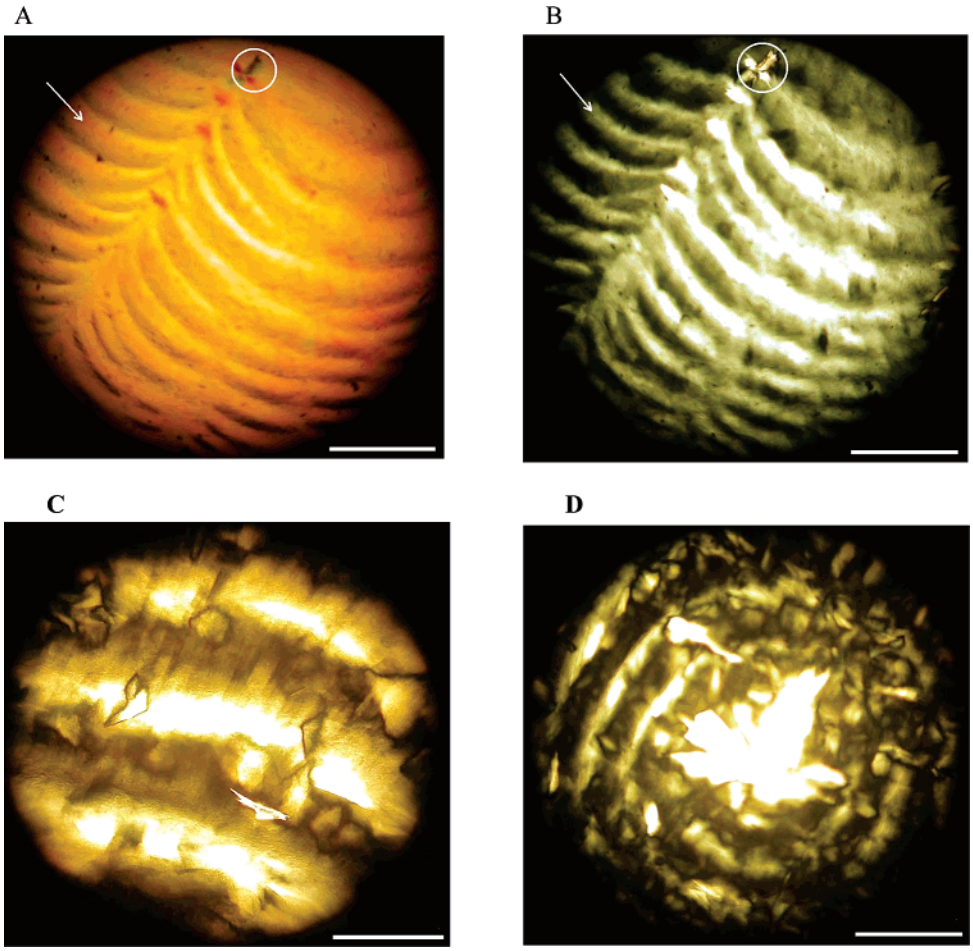

Figure 3. Photographs for patterns observed on polarizing optical microscope. (A) A part of a pattern under parallel-polarized light, the arrow points to a brighter stripe. (B) The same part of the pattern as that in (A) under perpendicular-polarized light; the arrow points to a bright stripe which is an anisotropic area and corresponds to that in (A). (C) A part of another pattern with larger size under perpendicular-polarized light. (D) The center of a concentric ring under perpendicular-polarized light. Scale bar 0.5 mm. A crystalline domain of residual surfactant is marked with a circle in (A) and (B).

rotated (Figure 4). As the polarizers were rotated (the angle between the two polarizers was varied from 0° to 90°), the concave regions in a pattern always correspond to the bright stripes, and the convex regions correspond to the dark stripes. This indicates that the dark stripes under perpendicular-polarized light are not the result of extinction due to orientation effects; instead, they represent the amorphous structure, while the bright stripes represent the ordered anisotropic structure.

Small-Angle X-ray Scattering Profiles. The investigations on ordered structures with small-angle X-ray scattering (SAXS) measurement are illustrated in Figure 5, in which the scattering intensities are given as a function of the scattering vector q (nm^{-1}). The SAXS measurements for Figure 5C (for concave valley) and Figure 5D (for convex ridge) were conducted with the sample with the largest macroscopic pattern (see Figure 2A macroscopic pattern formed at 20 °C), so the size of the focal spot of the X-ray beam (about 1 mm^2 in this study) can be comparable with or slightly less than that of the convex regions or concave regions. It is well-known that different microphase structures will exhibit different peak position ratios in the SAXS profile.[1,4−7] For examples, the body-centered-cubic (bcc) structure and the simple cubic structure have the same relative peak position ratios of $1:(2)^{1/2}:(3)^{1/2}:(4)^{1/2}:(5)^{1/2}:(6)^{1/2}$, the hexagonally packed cylindrical structure has the peak position ratios of $1:(3)^{1/2}:(4)^{1/2}:(7)^{1/2}$, and the lamellar structure has the peak position ratios of 1:2:3:4. A polymer−surfactant system can also exhibit multiple SAXS peaks due to its periodic microscopic structure having a long-range order. Information on the morphology can be obtained from the relative positions of these peaks. They can exhibit specific spatial relationships depending on the shape of the microdomain structure.[2,5,15−18] It can be seen from Figure 5A that for the pure surfactant there are three sharp peaks in the SAXS profile; the positions of these peaks are 3.31, 6.55, and 9.92 nm^{-1}, and this relative position of peaks is close to that of lamella structure. With the addition of a small amount of polymer (10 wt %) into the surfactant (Figure 5B), there were still three peaks in the SAXS profile with the peak positions similar to those of the pure surfactant, the relative intensity of the latter two peaks substantially decreased, and no new peak emerged, proving that small amount of polymer cannot form any new structure with the surfactant. As the amount of polymer was increased to 55 wt %, for the material in a concave region (Figure 5C), there were six peaks in the SAXS profile with their peak positions of 3.01, 3.32, 6.00, 6.66, 9.00, and 10.01 nm^{-1}, indicating that new structure was formed, and the scattering is generated by a superposition of two different lamellar systems: one with period around $2\pi/3.32$ nm and one with period around $2\pi/3.00$ nm (newly formed structure). While for the convex region (Figure 5D) in this sample, no peaks

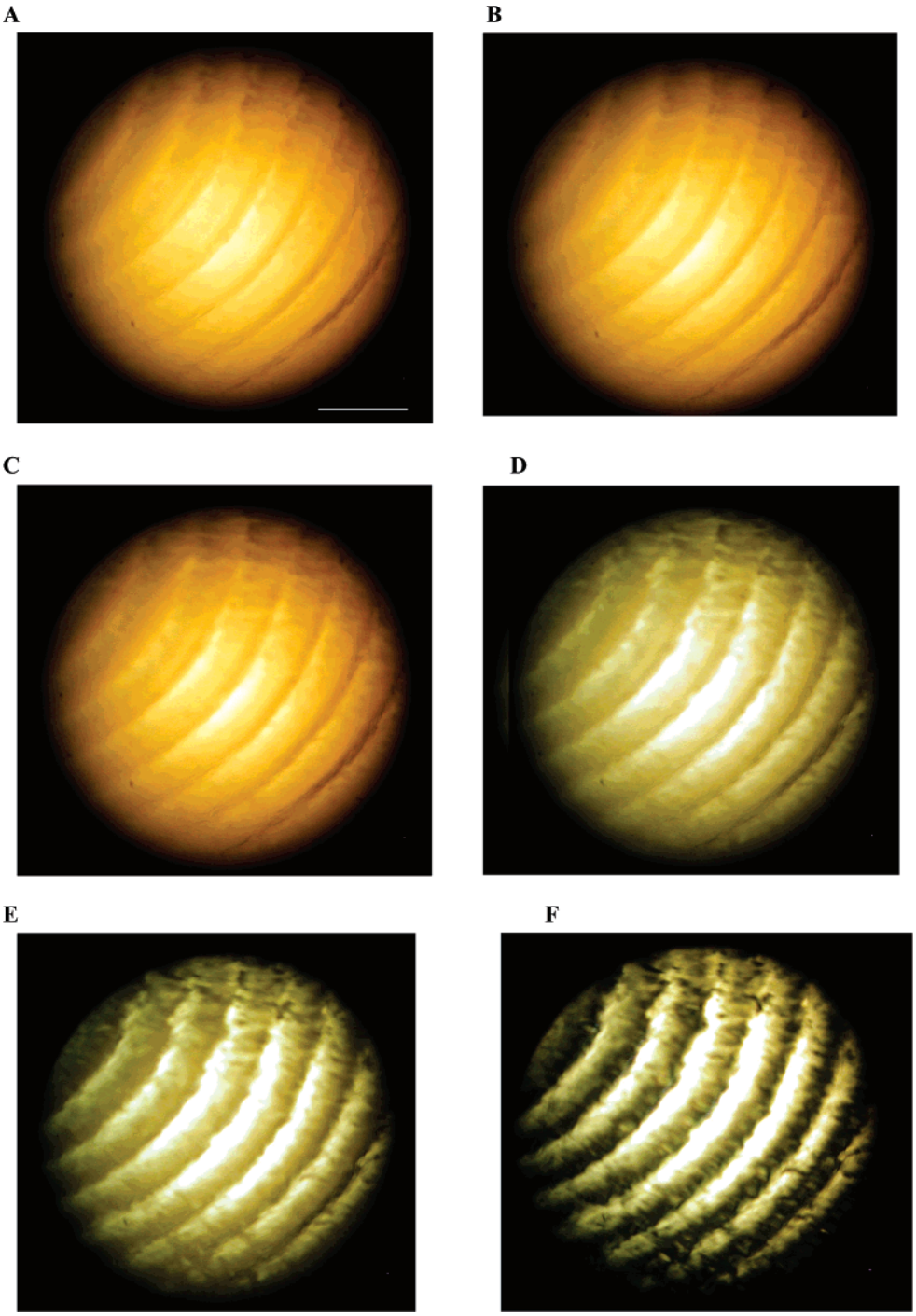

Figure 4. Photographs of a part of the pattern on polarizing optical microscope as the polarizers are rotated: (A) 0°, scale bar 0.5 mm; (B) 30°; (C) 45°; (D) 60°; (E) 75°; (F) 90°.

can be observed in the SAXS profile, indicating that the convex ridge in the macroscopic pattern mainly contains the amorphous region. We also found that further increase in polymer content to 80 wt % led to disappearance of all scattering peaks. The small-angle X-ray scattering investigations indicate that the ordered structure observed on the polarizing optical microscope is the mesomorphous phase formed by the surfactant chain packing in the polymer−surfactant system.

DSC Thermograms. The thermal properties of the polymer−TOAB systems were investigated by using DSC measurement. In Figure 6, endothermic transitions have been observed for pure surfactant as well as the polymer−TOAB systems (except for that with 90 wt % of polymer) during heating, which is due to melting of the octyl tail crystal. The pure TOAB shows a melting range of 95−101 °C with the melting peak at about 98 °C. We found the pure polymer exhibited no melting peak. At the polymer content of 10 wt %, the polymer−surfactant system shows a crystalline melting range of 87−101 °C with the melting peak at about 97 °C, which is close to that of the pure surfactant. At the polymer content of 55 wt %, the solid substance taken from the concave region (mesomorphous region) of the pattern exhibits a melting range of 84−99 °C with the melting peak at about 93.5 °C, and this melting peak shifts to lower temperature compared with that of pure TOAB. This melting peak shift indicates that the addition of

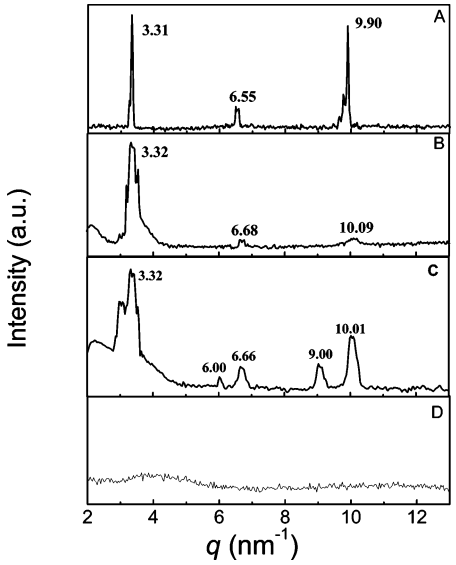

Figure 5. SAXS profiles for (A) pure surfactant TOAB cast from toluene, (B) the polymer−TOAB system cast from toluene with the polymer content of 10 wt %, (C) a concave region from the polymer−TOAB system with the polymer content of 55 wt %, and (D) a convex region from the polymer−TOAB system with the polymer content of 55 wt %.

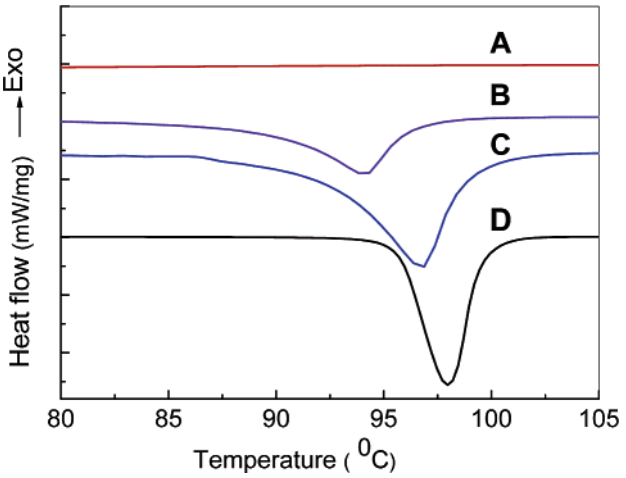

Figure 6. DSC thermograms of the polymer−surfactant TOAB systems and pure surfactant TOAB: A (red line), the polymer−surfactant system with the polymer content of 90 wt %; B (violet line), the polymer−surfactant system with the polymer content of 55 wt %; C (blue line), the polymer−surfactant system with the polymer content of 10 wt %; D (black line), pure surfactant.

polymer into surfactant affected the crystallization of the pure surfactant to some extent, and there is few pure surfactant crystalline phases or domains in the polymer−TOAB system with the polymer content of 55 wt %. Therefore, the ordered structure we observed in Figure 3 is the mesomorphous domain (or complex) formed by polymer and the surfactant, and the patterns we obtained were not caused by the phase separation of pure surfactant from the polymer.

Elemental Analysis and Phase Composition. To determine the composition for both the ordered and amorphous regions in the macroscopic pattern, we carefully took samples from the concave regions (ordered region) and convex (amorphous) regions respectively and determined the content of nitrogen element through elemental analysis; thus, the surfactant (TOAB) contents can be calculated for the two regions.

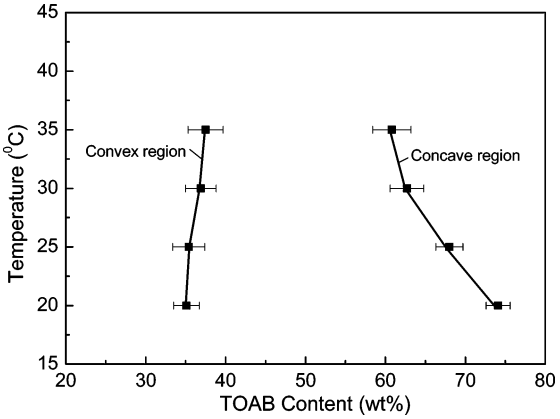

Figure 7. Phase composition curves: TOAB contents of the convex region and the concave region in the film with the polymer content of 55 wt % (TOAB content of 45 wt %). The data for higher temperatures cannot be obtained due to sampling difficulty. The error bar is presented for each point, which is the average of five measurement values.

As mentioned before, the pattern can only be obtained in a limited temperature range (20−45 °C), and the film cast at 45 °C has very thin patterns from which we cannot take samples, so we only determined the compositions for the films cast at 20, 25, 30, and 35 °C. To determine the TOAB content more accurately for a film cast at varied temperatures, we first prepared polymer/TOAB films under different temperatures; then in each film we took five samples (about 5 mg in weight each) from five different concave regions and then took another five samples from five different convex regions. Therefore, the TOAB contents as determined by elemental analysis for the concave region or the convex region in each film are the average of five measurements. The averaged values for TOAB contents in concave and convex regions in these solid films are shown in Figure 7.

From Figure 7, we can see that the convex regions are comprised of polymer-rich phase, while the concave regions are comprised of TOAB-rich phase. Therefore, we can say that the mesomorphous region observed under the polarizing microscope as shown in Figure 3 was mainly formed by the surfactant-rich materials, and the amorphous region was formed by the polymer-rich materials.

In Figure 7, as the film-forming temperature is increased, the surfactant content in the surfactant-rich phase (concave region) decreases, while that in the polymer-rich phase (convex region) increases. It can also be found from the figure that the change in TOAB content for convex region as a result of temperature variation is not as remarkable as that in the TOAB content for concave region (TOAB-rich phase). The reason for this is that the thickness contrast between the convex region and concave region for the film cast at higher temperature (about 2:1 for the one cast at 35 °C) is less than that of the film cast at lower temperature (about 3:1 for the one cast at 20 °C).

As for those poorly formed macroscopic patterns on the films, because of the small inter-ring spacing, the sampling from the concave or convex region in a film becomes extremely difficult, so the determination for the content of surfactant or the polymer is impossible. However, we can still anticipate that concave regions in those films were formed by surfactant-rich phase and the convex regions formed by polymer-rich phase.

Although we can obtain the composition for both the polymer-rich phase and the surfactant-rich phase of our prepared polymer/TOAB film, as shown in Figure 7, we suppose the data may not be able to represent the equilibrium composition for the polymer/TOAB system, since the composition of two phases is affected by both thermodynamic factors and kinetic factors. In general, the pattern formation is a solvent evaporation induced phase separation. Thermodynamically, during the evaporation of solvent, the polymer−surfactant interactions led to the formation of mesomorphous structures, and then phase separation occurred, which led to the formation of macroscopic pattern. Several processes can take place during evaporation of the solvent. One important thermodynamic factor affecting phase separation is the changes in the composition of the solution during the evaporation of solvent. As the solvent evaporates, the total composition of the mixture changes. At some specific composition of the mixture, the bionodal region in the phase diagram is passed and the region of incompatibility (spinodal region) is reached, and spinodal decomposition type phase separation occurs.[19]

On the other hand, the kinetic trapping of structures as a result of reduced mobility is also an important factor affecting the composition of the two phases.[20,21] Since the glass transition temperature T_g of the polymer (52 °C) and the melting point of the surfactant (98 °C) are all higher than the film-forming temperature (≤45 °C), as the solvent evaporated, the polymer chain segments and the surfactant molecules were gradually frozen as a result of the viscosity increase of the mixture, and eventually the phases are solidified and a film is formed. So for this solution-casting process, the resulting phase-separated morphology may be far from thermodynamic equilibrium, and relaxation toward equilibrium may be hindered by kinetic barriers formed by the nonequilibrium phase morphology.[20,21]

Therefore, because of the effect of solvent evaporation, the patterns obtained by solution-casting are not in thermodynamic equilibrium, although they are stable, kinetically "frozen" structures.

As for the film-forming temperature, it affects not only the composition of the two phases but also the evaporation rate of the solvent as well as the size of a single ring in the patterns. Increasing the temperature results in a decrease in the film formation time, and the viscosity of the solution dramatically increases; this produces a rapid quench of the polymer mixture, which "freeze" in a nonequilibrium phase separation morphology. Therefore, a single ring in a pattern has no time to grow to large size before its structure being frozen. On the other hand, at lower temperature, the film-forming time is longer, and a single ring in the patterns has time to grow to larger size. So, the size of the rings (domains) is determined by the complex interplay between the quench and the continuously decreasing mobility of the molecules, both caused by solvent evaporation.

As the temperature was further increased above 45 °C, the evaporation may be too fast, and the polymer chains and surfactant molecules have no time to move; thus, we cannot observe the pattern. On the other hand, as the temperature was reduced below 20 °C, we can only obtain a transparent film with no pattern on it. It is possible that as the solvent evaporates both the polymer chains and surfactant molecules can hardly move before the phase separation can take place.

Formation of Mesophase Structure. For the self-assembly of microscopic mesomorphous phases in the best-known polyelectrolyte−surfactant complex in water or high-polar solvents, the driving force is the electrostatic interaction, sometimes reinforced by hydrophobic interaction or hydrogen bond.[1,2,5] While in this study we obtained macroscopic mesomorphous phases by dissolving polymer and a structurally symmetrical surfactant in the low-polar solvent like toluene, thus the three interactions mentioned above are much weaker or even do not exist, since neither the polymer nor surfactant can ionize in toluene; however, there does exist polar interaction between polar groups in the system. The driving force(s) for the formation of mesomorphous region in this study is not quite clear, but we suppose they could be the van der Waals interactions between polymer chain and surfactant, and these interactions involve polar interactions and nonpolar interactions. The polar groups on the polymer side chains might interact with the polar groups of surfactant with the formation of joint associates, the interaction could also exist between the long thiophene-containing side chains and surfactant tails, and there also exist the steric (nonpolar) interactions between the alkyl tails of the surfactant and the polymer backbone.[1,4,22] These relatively weak interactions could probably lead to the formation of the mesomorphous structures of the surfactant−polymer system in the solid films. Furthermore, the fact that only the symmetrical surfactant with eight-carbon (C_8) tails can form macroscopic patterns implies that both the polar interactions and the nonpolar interactions are all critical to the formation of the mesomorphous structure. A delicate balance between these two kinds of interactions is necessary for this structure formation because the increase in the polar interaction by using surfactant TBAB (with four C_4 alkyl tails) or the increase in the nonpolar interaction by using surfactant TDAB (with four C_{12} alkyl tails) cannot lead to the formation of this mesomorphous structure as well as the macroscopic pattern.

Formation of Macroscopic Pattern. The photographs showing the formation process of the macroscopic patterns are listed in Figure 8. In the homogeneous solution of the TPA and TOAB system, as the solvent evaporated, first several nuclei of the concentric rings appeared, and then a ring formed around each nucleus after the formation of the nuclei; afterward, two rings formed for each concentric ring after the formation of the first ring; by this way the concentric rings continued to "grow"; finally, some concentric rings stopped to grow upon contact with one another. It can be concluded that the formation of each concentric ring, which makes up the macroscopic pattern, started from the center and then "grew" outward ring by ring.

In the polymer−surfactant solution, after the formation of the mesophase structure between the polymer and surfactant, as the solvent further evaporated, the unstable region (spinodal) in the phase diagram was reached, and phase separation occurred; consequently, surface undulation formed on the polymer−surfactant film. The following forces could be responsible for surface undulation: evaporation-induced convection[23,24] and/or the large interfacial tension between the surfactant−polymer mesomorphous phase and the polymer amorphous phase. Previously, researchers have also generated surface undulation (concentric rings) on dif-

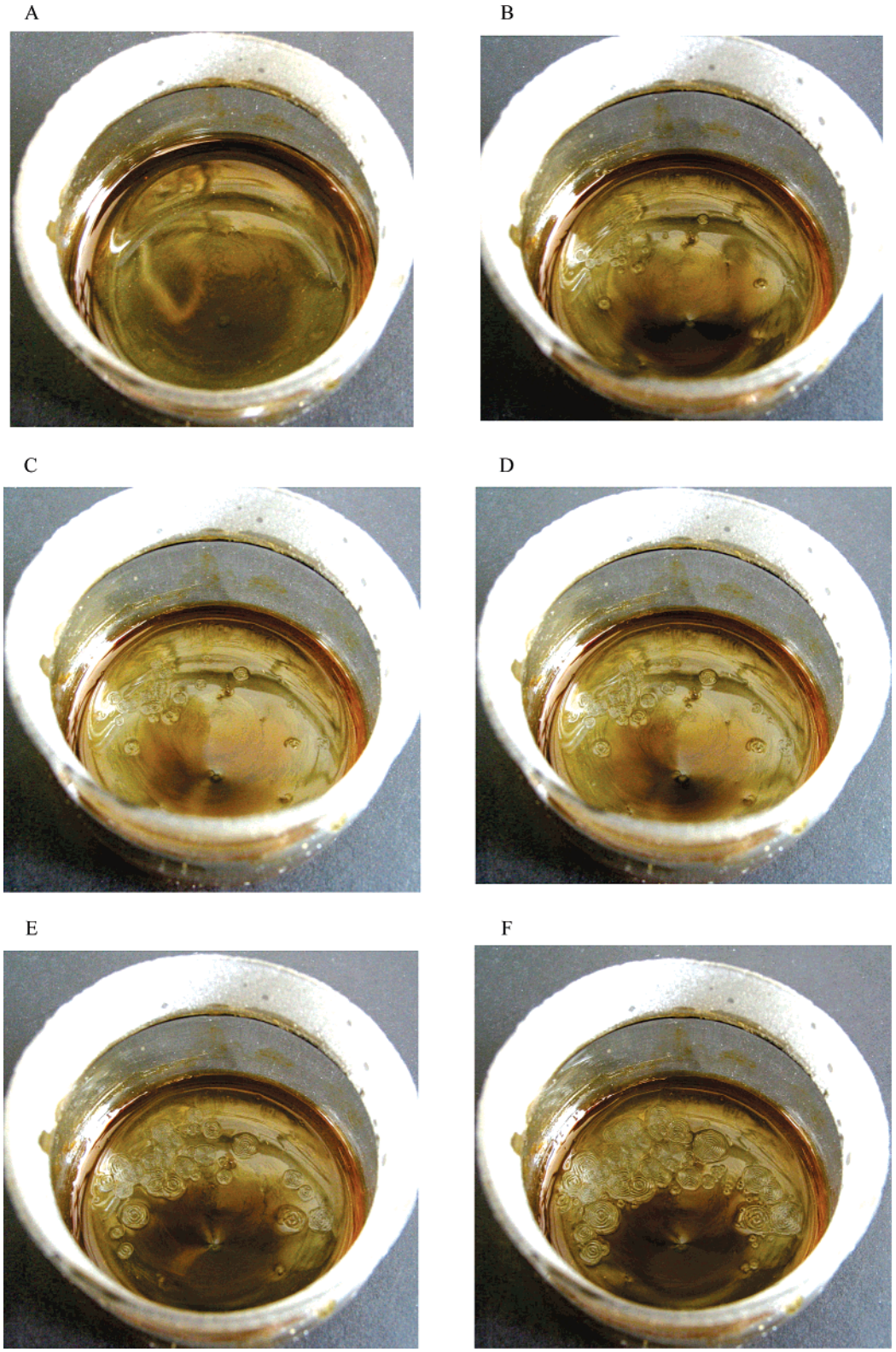

Figure 8. Photographs showing the formation process of the macroscopic pattern at the temperature of 35 °C (polymer content in the solid film is 55 wt %): (A) the homogeneous solution of the polymer and surfactant TOAB in toluene at the concentration of 6 wt % in a glass container; (B) about 60 min later, several nuclei of the concentric rings appeared; (C) a ring formed around each nucleus about 2 min after the formation of nuclei; (D) two rings formed for each concentric ring 3 min after formation of first ring; (E) concentric rings continued to "grow"; (F) some concentric rings stopped to grow upon contact with one another, at this stage more than half of the solvent remained in the system. The diameter of the glass container is about 4 cm.

ferent systems[23,24] (e.g., PS and PMMA or block copolymer) through evaporation convection, but no mesophase structure was involved in those convection patterns, and usually no surfactants were added to those systems. Some other researchers have generated spiral patterns (usually in microscopic scale) in liquid crystal polymers or biomacromolecules.[25,26] Hydrogen bonding is mainly responsible for appearance of the spiral patterns in biomacromolecules, while the interaction between disclinations is the main cause of the spiral patterns in

liquid crystal polymers.[25,26] Hence, the formation mechanism of spiral patterns is different from that of the concentric macroscopic patterns in our polymer−surfactant system. In our case, a large amount of surfactant was involved in the formation of the macroscopic pattern, and the formation of the mesophase structure could also be critical to the patterning; the macroscopic pattern can only be obtained under specific conditions. For example, macroscopic patterns can only be generated in those TPA−TOAB systems that form the mesophase structure; no patterns can be formed by the polymer with other surfactants with similar structure as that of TOAB such as tetrabutylammonium bromide and tetradodecylammonium bromide, and the removal of the thiophene-containing pendant groups results in the disappearance of macroscopic patterns. Our polymer−TOAB−organic solvent is a new system that can form macroscopic patterns.

On the basis of the above investigations and observations, we propose the following pattern formation process. Upon addition of polymer and surfactant into some organic solvent like toluene, a ternary homogeneous solution was formed. As the solution was cast on the glass substrate and with the evaporation of some organic solvent, the interaction between the solvent and some solute molecules substantially decreased, and the surfactant-rich mesomorphous structures were thereby formed by some surfactant and polymer molecules driven by van der Waals interactions which include polar interactions and nonpolar interactions, and then the system was turned from the one-phase stable region into the unstable region. Phase separation seems to occur through spinodal decomposition. At this point concentration fluctuations become unstable and grow, rather than decay, giving domains rich in one species; by this way the mesomorphous domains phase-separated from the solution and gradually constituted the nuclei of the concentric rings (Figures 3D and 8). At this time, the amorphous domains might form around each nucleus and constitute a ring because the center had been occupied. As the evaporation went on, another mesomorphous ring formed around the former amorphous ring, and then this process continued until the motion of polymer chains were frozen due to the solvent evaporation. The convection and/or the capillary forces due to the interfacial tension on both sides of the amorphous ring might "push" the polymer-rich amorphous phase to protrude and eventually form the circular ridge. In addition, we think the molecular chain motion of both the polymer and the surfactant is also important to the pattern formation. As evidenced by our observation that the solvent evaporation at lower temperature or using higher boiling point solvent can all result in larger and well-formed pattern, the slow solvent evaporation makes the solvent leave more slowly; hence, the molecular chain motion could have enough time to move and settle to form the ordered pattern during the phase separation.

Conclusions

The highly ordered mesomorphous structure can also be obtained from the polymer (nonpolyelectrolyte) and surfactant system with no strong interaction involved, and this unique microscopic ordering can cause macroscopic patterns in solid state. A macroscopic pattern is alternatively organized by circular convex ridges and concave valleys, with the former being the polymer-rich amorphous phase and the latter being the surfactant-rich mesomorphous phase. The formation of the macroscopic patterns involves three processes: (1) formation of mesoscopic structure, (2) phase separation, and (3) surface undulation. This macroscopic patterning in the solid polymer−surfactant system could offer a new way for fabricating ordered supramolecular structure in macroscopic dimensions.

Acknowledgment. This work was supported by NSFC (Project No. 50573023 and 50473035), NSFG (No. 04020043), and NCET.

Supporting Information Available: Monomer synthesis scheme, FTIR spectra, and ^{1}H NMR spectra. This material is available free of charge via the Internet at http:// pubs.acs.org.

References and Notes

(1) Kotz, J.; Kosmella, S.; Beitz, T. *Prog. Polym. Sci.* **2001**, *26*, 1199−1232.
(2) Zhou, S. Q.; Chu, B. *Adv. Mater.* **2000**, *12*, 545−556.
(3) Muthukumar, M.; Ober, C. K.; Thomas, E. L. *Science* **1997**, *277*, 1225−1232.
(4) Thunemann, A. F. *Adv. Mater.* **1999**, *11*, 127−130.
(5) Thunemann, A. F. *Prog. Polym. Sci.* **2002**, *27*, 1473−1572.
(6) Thunemann, A. F.; Muller, M.; Dautzenberg, H.; Joanny, J. F.; Lowen, H. *Adv. Polym. Sci.* **2004**, *166*, 113−171.
(7) Zhou, S. Q.; Hu, H. B.; Burger, C.; Chu, B. *Macromolecules* **2001**, *34,* 1772−1778.
(8) Norenberg, R.; Klingler, J.; Horn, D. *Angew. Chem., Int. Ed.* **1999**, *38*, 1626−1629.
(9) Yeh, F. J.; Sokolov, E. L.; Khokhlov, A. R.; Chu, B. *J. Am. Chem. Soc.* **1996**, *118,* 6615−6618.
(10) Zhou, S. Q.; Liang, D. H.; Burger, C.; Yeh, F. J.; Chu, B. *Biomacromolecules* **2004**, *5*, 1256−1261.
(11) Kurth, D. G.; Meister, A.; Thunemann, A. F.; Forster, G. *Langmuir* **2003**, *19*, 4055−4057.
(12) Thunemann, A. F.; Kubowicz, S.; Burger, C.; Watson, M.; Tchebotareva, N.; Mullen, K. *J. Am. Chem. Soc.* **2003**, *125*, 352−356.
(13) Antonietti, M.; Conrad, J.; Thunemann, A. *Macromolecules* **1994**, *27*, 6007−6011.
(14) Antonietti, M.; Maskos, M. *Macromolecules* **1996**, *29*, 4199−4205.
(15) Merta, J.; Garamus, V. M.; Willumeit, R.; Stenius, P. *Langmuir* **2002**, *18,* 7272−7278.
(16) Thunemann, A. F.; General, S. *Macromolecules* **2001**, *34*, 6978−6984.
(17) Thunemann, A. F.; Kubowicz, S.; Pietsch, U. *Langmuir* **2000**, *16*, 8562−8567.
(18) Chu, B.; Hsiao, B. S. *Chem. Rev.* **2001**, *101,* 1727−1761.
(19) Henderson, I. C.; Clarke, N. *Macromolecules* **2004**, *37,* 1952−1959.
(20) Petersson, M.; Loren, N.; Stading, M. *Biomacromolecules* **2005**, *6,* 932−941.
(21) Walheim, S.; Bo1tau, M.; Mlynek, J.; Krausch, G.; Steiner, U. *Macromolecules* **1997**, *30,* 4995−5003.
(22) Hsiao, M. S.; Chen, H. L.; Liaw, D. J. *Macromolecules* **2000**, *33*, 221−224.
(23) Mitov, Z.; Kumacheva, E. *Phys. Rev. Lett.* **1998**, *81*, 3427−3430.
(24) Sakurai, S.; Tanaka, K.; Nomura, S. *Macromolecules* **1992**, *25*, 7066−7068.
(25) Zhang, S.; Eugene, M. T.; Donald, A. M. *Macromolecules* **2004**, *37*, 390−396.
(26) Kurihara, S.; Mori, T.; Nonaka, T. *Macromolecules* **1998**, *31*, 5940−5942.

MA051042G